
The Cross-environment Hyperparameter Setting Benchmark for Reinforcement Learning

Andrew Patterson, Samuel Neumann, Raksha Kumaraswamy, Martha White, Adam White
Department of Computing Science, University of Alberta
{ap3, sfneuman, kumarasw, whitem, amw8}@ualberta.ca

Abstract

1 This paper introduces a new benchmark, the Cross-environment Hyperparameter
2 Setting Benchmark, that allows comparison of RL algorithms across environments
3 using only a single hyperparameter setting, encouraging algorithmic development
4 which is insensitive to hyperparameters. We demonstrate that the benchmark is
5 robust to statistical noise and obtains qualitatively similar results across repeated
6 applications, even when using a small number of samples. This robustness makes
7 the benchmark computationally cheap to apply, allowing statistically sound insights
8 at low cost. We provide two example instantiations of the CHS, on a set of six
9 small control environments (SC-CHS) and on the entire DM Control suite of 28
10 environments (DMC-CHS). Finally, to demonstrate the applicability of the CHS to
11 modern RL algorithms on challenging environments, we provide a novel empirical
12 study of an open question in the continuous control literature. We show, with
13 high confidence, that there is no meaningful difference in performance between
14 Ornstein-Uhlenbeck noise and uncorrelated Gaussian noise for exploration with
15 the DDPG algorithm on the DMC-CHS.

16 1 Introduction

17 One of the major benefits of the Atari suite is the focus on more general reinforcement learning agents.
18 Numerous agents have been shown to exhibit learning across many games with a single architecture
19 and a single set of hyperparameters. To a lesser extent, OpenAI Gym (Brockman et al., 2016) and DM
20 control suite (Tassa et al., 2018) are used in the same way—though at times not all environments are
21 used, raising the possibility of cherry-picking. As the ambitions of the community have grown, Atari
22 and OpenAI Gym tasks have been combined into larger problem suites, with subsets of environments
23 chosen to test algorithms. In many ways we are back to where we started with Cartpole, Mountain
24 Car and the like: where environment-specific hyperparameter tuning and problem subselection is
25 prominent. Instead of proposing a new and bigger challenge suite, we explore a challenging new
26 benchmark and empirical methodology for comparing agents across a given set of environments,
27 complementing the existing empirical toolkit for investigating the scalability of deep RL algorithms.

28 In order to make progress towards impactful applications of reinforcement learning and the broader
29 goals of AGI, we need benchmarks that clearly highlight the generality and stability of learning
30 algorithms. Empirical work in Atari, Mujoco, and simulated 3D worlds typically use networks with
31 millions of parameters, dozens of GPUs, and up to billions of samples (Beattie et al., 2016; Espeholt
32 et al., 2018). Many results are demonstrative, meaning that the primary interest is not the stability
33 and sensitivity, nor what was required to achieve the result, rather that the result *could* be achieved.
34 It is infeasible to combine these large scale experiments with hyperparameter studies and enough
35 independent runs to support statistically significant comparisons. More evidence is emerging that
36 such state of the art systems (1) rely on environment-specific design choices that are sensitive to
37 minor changes to hyperparameters (Henderson et al., 2018; Engstrom et al., 2019), (2) are less data

38 efficient and stable compared with simple baselines (van Hasselt et al., 2019; Taïga et al., 2019),
 39 and (3) cannot solve simple toy tasks without extensive re-engineering (Obando-Ceron and Castro,
 40 2021; Patterson et al., 2021). It is abundantly clear that modern RL methods can be adapted to a
 41 broader spectrum of challenging tasks—well beyond what was possible with linear methods and
 42 expert feature design. However, we must now progress to phase two of empirical deep RL research:
 43 focusing on generality and stability.

44 There is a growing movement to increase the standards of empirical work in RL. Noisy results,
 45 inconsistent evaluation practices, and divergent code bases have fueled calls for more open-sourcing
 46 of agent architecture code, experiment checklists, and doing more than three independent evaluations
 47 in our experiments (Henderson et al., 2018; Pineau et al., 2020). Digging deeper, recent work has
 48 highlighted our poor usage of basic statistics, including confidence intervals and hypothesis tests
 49 (Colas et al., 2018). Long before the advent of deep networks, researchers called out the environment
 50 overfitting that is rampant in RL and proposed sampling from parameterized variants of classic
 51 control domains to emphasize general methods (Whiteson et al., 2009). Finally, and most related to
 52 our work, Jordan et al. (2020) proposed a methodology to better characterize the performance of an
 53 algorithm across environments, evaluated with randomly sampled hyperparameters. We build on this
 54 direction, but focus on a simpler and more computationally frugal evaluation that examines the single
 55 best hyperparameter setting across environments, rather than a randomly sampled one, and allows for
 56 a smaller number of runs per environment.

57 Table 1: Chance of incorrect claims

	3 runs	10	30	100
58 Acrobot	47%	31%	22%	1%
59 Cartpole	7%	0%	0%	0%
60 CliffWorld	54%	19%	14%	0%
61 LunarLander	16%	7%	1%	0%
62 MountainCar	22%	9%	7%	0%
63 PuddleWorld	18%	16%	8%	0%

64 One reason we focus on computational efficiency is that computational limitations seems to be the pri-
 65 mary culprit for misleading or incorrect claims in RL experiments. Experiments with many runs, many hy-
 66 perparameters, and many environments can be computationally prohibitive. The typical trade-off is to
 67 use a smaller number of runs. Such a choice, however, can lead to incorrect conclusions. Table 1 shows
 68 the empirical probability of incorrectly ordering four
 69 reasonable RL algorithms across several domains often considered too small to draw meaningful con-
 70 clusions. We ran each of the four algorithms 250 times on every domain and for every hyperparameter
 71 setting in an extensive sweep to get a high confidence approximation of the correct ordering between
 72 algorithms. We then used bootstrap sampling to simulate 10k papers—each using a small number of
 73 random seeds—and counted the frequency that incorrect algorithm orderings were reported. Even
 74 with 30 runs in these small domains, incorrect rankings were **not** uncommon. Further details are
 75 described in Section 5.

76 Another critical issue for algorithm evaluation is the difficulty in hyperparameters selection. Modern
 77 RL algorithms require tuning an increasing number of hyperparameters, greatly impacting the
 78 outcome of an experimental trial. As more hyperparameters are introduced, the computational
 79 burden of tuning grows exponentially. To combat this, several strategies have emerged in the literature
 80 including relying on default hyperparameter values (Schaul et al., 2016; Wang et al., 2016; Van Hasselt
 81 et al., 2016), tuning hyperparameters on a subset of domains (Bellemare et al., 2013), or eroding
 82 standards of sufficient statistical power for publication (Henderson et al., 2018; Colas et al., 2018).

83 Our new benchmark is designed to (1) standardize the selection of hyperparameters, (2) evaluate
 84 stability over runs, (3) be computationally cheap to run, and (4) be easy to use. We propose the Cross-
 85 environment Hyperparameter Setting Benchmark (CHS). The basic idea is simple: an algorithm is
 86 evaluated on a set of environments, using the best hyperparameter setting across those environments,
 87 rather than per-environment. Though conceptually simple, this methodology is not widely used.
 88 We first address some of the nuances in the CHS, namely how to standardize performance across
 89 environments to allow for aggregation, how to allow for robust measures of performance, and finally
 90 how to reduce computation to make it more feasible to use the CHS. We evaluate the effectiveness of
 91 the CHS itself by examining the stability of the conclusions from the CHS under different numbers
 92 of runs. We then demonstrate that the CHS can result in different conclusions about algorithms
 93 compared to the conventional *per-environment tuning* approach and the more recent approach of
 94 using a subset of environments for tuning. We conclude with a larger demonstration of the CHS on
 95 DM Control Suite.

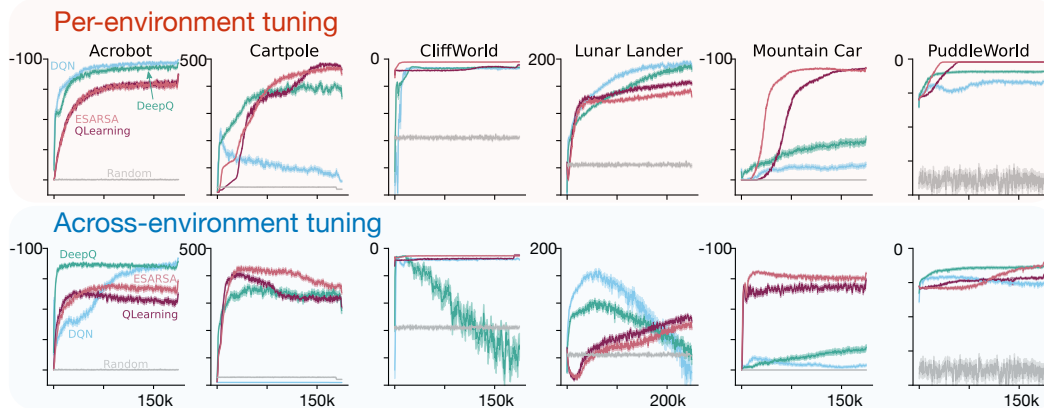
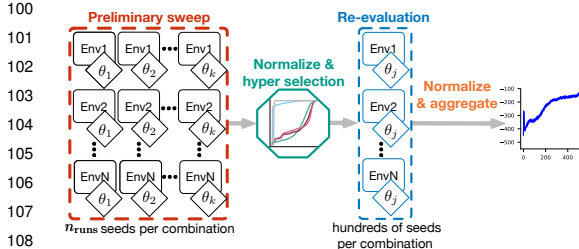


Figure 1: An example experiment comparing four algorithms across six different environments. Each learning curve shows the mean and standard error of 250 independent runs for each algorithm and environment. Hyperparameters are selected using three runs of every algorithm, environment, and hyperparameter setting. **Top** shows the learning curves when the best hyperparameters are chosen for each environment individually. **Bottom** shows the learning curves when hyperparameters are chosen according to our benchmark, the CHS.

93 2 Contrasting Across-Environment versus Per-Environment Tuning

94 In this section, we introduce the basic procedure for the CHS and provide an experiment showing
 95 how it can significantly change empirical outcomes compared to the conventional per-environment
 96 tuning approach. We provide specific details for each step later and here focus on outlining the basic
 97 idea and its utility.

98 The CHS consists of the following four steps summarized in the inset figure below. We assume we
 99 are given a set of environments and a set of hyperparameters for the algorithm we are evaluating.



Step 1 (Preliminary Sweep) Run the algorithm for all hyperparameters and all environments, for n_{runs} runs (i.e., $n_{\text{runs}} < 30$) and record the performance of every combination. The performance could be online average return per step.

Step 2 (Normalization) Normalize the scores across environments to be in $[0, 1]$. We use CDF normalization, which is described in Section 4.

Step 3 (Hyperparameter Selection) Select the hyperparameter setting with the highest score averaged across environments.

109 **Step 4 (Re-evaluation)** With the single best hyperparameter setting, use many more runs in each
 110 environment (e.g. 100) to produce a more accurate estimate of performance.
 111

112 The last step is more lightweight than it appears since only a single hyperparameter setting is used
 113 for all environments. Executing 100 or more runs for every hyperparameter setting would likely be
 114 prohibitive. The trick is to use a small n_{runs} in the Preliminary Sweep, saving compute, and a larger
 115 number of runs in the Re-evaluation step. This contrasts the conventional *per-environment tuning*
 116 approach of choosing hyperparameter settings which maximize performance on each environment
 117 individually, which can be more sensitive when n_{runs} is small.

118 We now show an experiment comparing the CHS and this conventional approach in Figure 1. The
 119 per-environment tuning approach highlights the ideal behavior of an algorithm per environment,
 120 whereas the CHS highlights the (in)sensitivity of an algorithm across environments. Experimental
 121 details can be found in Section 5. The environments are relatively simple (most coming from the
 122 classic control suite of OpenAI Gym (Brockman et al., 2016)) but difficult enough for our purposes:
 123 no one algorithm could reach near optimal performance in all environments.

124 The CHS does not rank the algorithms differently than with per-environment tuning, but CHS
 125 does alert us to potential catastrophic failure of some algorithms. The neural network DeepQ
 126 agent performs terribly in Cliffworld and Lunar Lander under CHS, but appears reliable under
 127 the per-environment approach. What is going on? Forced to select only one hyperparameter

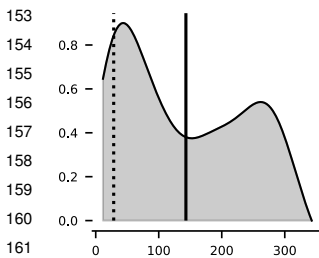
128 across environments, the best outcome is to sacrifice performance in Cliffworld and Lunar Lander—
129 achieving worse performance than a uniform random policy.

130 3 Performance Distributions

131 In this section, we describe the distribution and random variables underlying an RL experiment. This
132 formalism allows us to reason about the summary statistics we consider for the CHS in the next
133 section. We also visualize these distributions to provide intuition on the properties of the summary
134 statistics of these distributions and the implications for the single performance numbers used in RL.

135 In an RL experiment, we seek to describe the performance distribution of an algorithm for each
136 hyperparameter setting $\theta \in \Theta$, denoted as $\mathbb{P}(G, E | \theta)$ where G is a random variable indicating
137 the performance of an algorithm on a given environment, $E \in \mathcal{E}$. Most commonly, we report
138 an estimate of the average performance conditioned on environment and hyperparameter setting,
139 $g(E, \theta) \cong \mathbb{E}[G | E, \theta]$ using a sample average and some measure of uncertainty about how accurately
140 $g(E, \theta)$ approximates $\mathbb{E}[G | E, \theta]$.

141 The environment can be seen as a random variable for many RL experiments. The most common
142 case is to specify a set of MDPs that the authors believe represent the important applications of their
143 new algorithm. If results are uniformly aggregated across these environments, then this corresponds
144 to assuming a uniform distribution over this set of environments. Other times, random subsets of
145 environments from environment suites are chosen; the performance estimate on this subset provides
146 an estimate of performance across the entire suite. The idea of evaluating algorithms over a random
147 sample of MDPs has been studied explicitly previously. For example, the parameters determining
148 the physics of classical control domains were randomized and sampled to avoid domain overfitting
149 (Whiteson et al., 2009), and randomly generated MDPs (Archibald et al., 1995) have been used to
150 evaluate new algorithmic ideas (Seijen and Sutton, 2014; Mahmood et al., 2014; White and White,
151 2016). If we subselect after running the algorithms, then we bias the distribution over environments
152 towards those with higher performance.



153
154
155
156
157
158
159
160
161
162
163 Figure 2: Performance
164 distribution $\mathbb{P}(G | E, \theta)$
165 on Cartpole with hyper-
166 parameter $\text{stepsize}=2^{-9}$.

Let us look at an example of these performance distributions to gain some
intuition for estimating statistics like the expected performance. Consider the action-value nonlinear control method DQN, using the Adam optimizer (Mnih et al., 2013; Kingma and Ba, 2015), on Cartpole (Barto et al., 1983). We fix the hyperparameter setting θ to the default values from Raffin et al. (2019). For this fixed environment, all randomness is due to sampling algorithm performance on this environment, namely sampling G according to $\mathbb{P}(G | E, \theta)$. The performance, G , is the average episodic return over all episodes completed during 100k learning steps. This environment is considered solved for $G > 400$. We repeat this procedure for 250 independent trials to estimate the distribution $\mathbb{P}(G | E, \theta)$, shown in Figure 2, with x-axis possible outcomes of G and y-axis the probability density. The vertical solid line denotes mean performance, and the vertical dotted line denotes mean performance of a random policy.

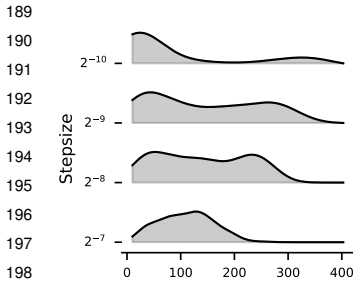
167 Figure 2 is a typical example of the performance of an RL algorithm over multiple independent
168 trials. In this case, DQN is more likely to fail than to learn a policy which solves this relatively
169 simple environment. It is common practice to run an RL algorithm for some number of random
170 seeds—effectively drawing samples of performance from this distribution—then reporting the mean
171 over those samples (solid vertical line).

172 There are two implications from observing this bimodal performance distribution. First, using the
173 expected value of this distribution as the summary statistic does not aptly demonstrate that the poor
174 performance of DQN on Cartpole is due to occasional catastrophic failure—performing worse than
175 or equivalent to a random policy. Instead, mean performance might lead us to wrongly conclude that
176 DQN on Cartpole usually finds a sub-optimal, yet better than random, policy. An alternative might
177 be to consider percentile statistics or, if the goal is to evaluate mean performance, to avoid drawing
178 strong conclusions about individual runs.

179 If the goal is to report mean performance, then a second issue arises. Estimating the mean of these
180 non-normal performance distributions can be challenging. In Figure 2, approximately 70% of the

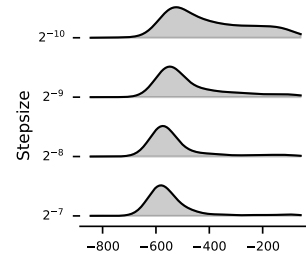
181 density is around a mode centered at 20 return, and the remaining 30% is around a mode centered at
 182 250 return. As a result, sample means constructed with only three runs are varied and skewed.

183 Further, to report the average performance of the best performing hyperparameter—that is
 184 $\max_{\theta \in \Theta} \mathbb{E}[G \mid \theta, E]$ —we must first reliably estimate the conditional expected performance for
 185 each hyperparameter. Computing this expectation can require a large number of samples to obtain a
 186 reasonable estimate for each hyperparameter. This results in a tradeoff between measuring sensitivity
 187 and stability: between the breadth of hyperparameter settings that can be studied and the accuracy to
 188 with which we can feasibly evaluate each hyperparameter.



The summary statistic used to select hyperparameters also interacts with the form of the performance distribution. In the inset figure on the left we show the performance distribution across four different choices of stepsize parameter of DQN in **Cartpole**. If we are interested only in the highest best case performance, then 2^{-10} is preferred. However, if we are particularly concerned with reducing the chances of catastrophic failure (i.e., highest worst case performance), then a stepsize 2^{-7} is preferred. The most common case is to report results for the stepsize with the highest average performance. In this case, a stepsize of 2^{-9} would be preferred.

199 These performance distributions can also look quite different for differ-
 200 ent environments, even with the same algorithm. For Cartpole (above),
 201 the distribution is increasingly long-tailed with smaller stepsizes. For
 202 **Puddle World**, shown in the inset figure on the right, the distributions
 203 are always bimodal with one mode around -600 return and a second
 204 mode around -200 return. With smaller stepsizes, the density around
 205 the better performance mode increases, shifting the mean of the distri-
 206 bution. Peak performance does not change; rather the probability that
 207 DQN has a good run is higher with small stepsizes. This analysis of
 208 performance distributions raises an important question: do current RL
 209 algorithms have consistent hyperparameter settings which perform well across many environments?



210 4 The Cross-environment Hyperparameter Setting Benchmark

211 In this section, we describe our new benchmark for evaluating RL algorithm across environments, the
 212 Cross-environment Hyperparameter Setting Benchmark (CHS). Although it seems natural to evaluate
 213 across environments, standard empirical practice in RL is not done this way. Understanding across-
 214 environment sensitivity aligns nicely with the intent of sensitivity analysis: elucidating how well an
 215 algorithm might perform on new environments without extensive hyperparameter tuning. We argue
 216 that the CHS 1) better aligns empirical practice with the goals of applied RL, 2) is computationally
 217 feasible even in complex environments, 3) provides novel insights on old ideas (even with small
 218 environments), and 4) reduces the chances of accidentally publishing incorrect conclusions due to
 219 statistical noise.

220 We now reiterate the procedure for the CHS with more details than the high-level procedure given
 221 in Section 2. The first step (**preliminary sweep**) is to draw a small number of samples n_{runs} from
 222 $\mathbb{P}(G \mid \theta, E)$ for every hyperparameter setting and environment and get the summary estimate $g(E, \theta)$
 223 from those samples. Typically, we compute $g(E, \theta)$ as a sample average to estimate $\mathbb{E}[N_E(G) \mid E, \theta]$,
 224 where $N_E : \mathbb{R} \rightarrow \mathbb{R}$ is a **normalization** function that we describe below. Then we aggregate across
 225 environments to estimate $g(\theta) \approx \mathbb{E}[\mathbb{E}[N_E(G) \mid E, \theta]]$, where the outer expectation is with respect
 226 to environments. Then we **select** a single hyperparameter setting with $\theta_{\text{CHS}} = \arg \max_{\theta \in \Theta} g(\theta)$.
 227 Finally, we draw a large number of samples from $\mathbb{P}(G \mid \theta_{\text{CHS}}, E)$ for every environment and report
 228 the same summary statistics $g(E, \theta_{\text{CHS}})$ and $g(\theta_{\text{CHS}})$ (**re-evaluation**).

229 In order to compute the expectation over environments we must normalize the performance measures.
 230 Generally, we cannot expect each environment to produce normalized performance numbers. A
 231 comprehensive discussion of normalization methods is given in Jordan et al. (2020). We use a lightly
 232 modified version of the CDF normalization method from Jordan et al. (2020), $N_E(G) = \text{CDF}(G, E)$,
 233 which is itself an instance of probabilistic performance profiles (Barreto et al., 2010).

234 We first collect the performance of each algorithm, environment, and hyperparameter tuple. Then,
 235 let \mathcal{P}_E be the pool of performance statistics g for every agent—namely a run of each algorithm and
 236 hyperparameter pair—for a given environment E . Our goal is to take a given agent’s performance
 237 $x \in \mathcal{P}_E$ and return a normalized performance. The CDF normalization, for this x in this environment,
 238 is

$$\text{CDF}(x, E) = \frac{1}{|\mathcal{P}_E|} \sum_{g \in \mathcal{P}_E} \mathbf{1}(g < x)$$

239 where $\mathbf{1}$ is the indicator function. This mapping says: what percentage of performance values, across
 240 all runs for all algorithms and all hyperparameter settings, is lower than my performance x on this
 241 particular environment E ? For example, if $\text{CDF}(x, E) = 0.25$, then this agent’s performance is
 242 quite low in this environment, as only 25% of other agents’ performance was worse and 75% was
 243 higher, across agents tested. This normalization accounts for the difficulty of the problem, and reflects
 244 relative performance amongst agents tested. Note that this normalization uses an empirical CDF,
 245 rather than the true CDF for the environment and set of hyperparameters and agents. This means
 246 there is a small amount of bias when estimating $\mathbb{E}[\mathbb{E}[N_E(G) \mid E, \theta]]$. This bias dissipates with an
 247 increasing numbers of samples and equally impacts all compared algorithms.

248 Selecting hyperparameters with the CHS can require significantly fewer samples compared with
 249 conventional per-environment tuning. Per-environment tuning requires a sufficiently accurate estimate
 250 of the conditional expectation $\mathbb{E}[G \mid E, \theta]$ for every $\theta \in \Theta$ and for every $E \in \mathcal{E}$, requiring a number
 251 of runs proportional to $|\Theta||\mathcal{E}|$. The CHS, on the other hand, requires only an accurate estimate of
 252 $\mathbb{E}[N_E(G) \mid \theta] = \mathbb{E}[\mathbb{E}[N_E(G) \mid E, \theta]]$ which requires a number of runs proportional only to $|\mathcal{E}|$. By
 253 designing a process which selects hyperparameters first using a smaller number of runs, we can
 254 reserve more computational resources for re-evaluation. Once we select the best hyperparameters,
 255 the cost of collecting samples is independent of Θ , and so we can decouple the precision of our
 256 performance estimate from the number of hyperparameter settings that we evaluate for each algorithm.

257 Finally, we can contrast this benchmark with a recent evaluation scheme that uses random hy-
 258 perparameter selection (Jordan et al., 2020). In order to capture variation in performance due to
 259 hyperparameter sensitivity, Jordan et al. (2020) treats hyperparameters as random variables and
 260 samples according to an experimenter-designated distribution over hyperparameters, reporting the
 261 mean and uncertainty with respect to this added variance, similar to the procedure used in Jaderberg
 262 et al. (2016). This evaluation methodology provides some insight into the difficulty of tuning, though
 263 requires a sensible distribution over hyperparameters to be chosen. The CHS, on the other hand, asks:
 264 is there a hyperparameter setting for which this algorithm can perform well across environments? It
 265 motivates instead identifying that single hyperparameter, and potentially fixing it in the algorithm, or
 266 suggesting that the algorithm needs to be improved so that such a hyperparameter could feasibly be
 267 found. Both of these strategies help identify algorithms that are difficult to tune, but the CHS is easier
 268 to use and computationally cheaper.

269 5 Evaluating the Cross-environment Hyperparameter Setting Benchmark

270 In this section, we evaluate the CHS by comparing four algorithms across several classic control
 271 environments. For this evaluation, we require environments where hundreds of independent samples
 272 of performance can be drawn across a large hyperparameter sweep in a computationally tractable
 273 way. We emphasize that this is not a general requirement of the CHS and is required only in this
 274 case of evaluating the CHS’s responsiveness to perturbations in the experimental process. Because
 275 these classic control environments are cheap to run and provide meaningful insights in differentiating
 276 modern RL algorithms (Obando-Ceron and Castro, 2021), we name this specific benchmark the
 277 Small Control CHS (SC-CHS). In Section 6 we provide a realistic demonstration of the CHS on a
 278 larger dataset with a more complex algorithm.¹

279 For the following investigations, we compare two deep RL algorithms based on DQN (Mnih et al.,
 280 2013) and two control algorithms based on linear function approximation using tile-coded features
 281 (Sutton and Barto, 2018). The deep RL algorithms, DQN and DeepQ, differ only in their loss: DQN
 282 uses a clipped loss and DeepQ uses a mean squared error. For the two tile-coding agents, QLearning
 283 is off-policy and bootstraps using the greedy action, while ESARSA is on-policy and bootstraps using
 284 an expectation over actions. Further details on the algorithms can be found in Appendix C.

¹All code can be found at <https://github.com/andnp/single-hyperparameter-benchmark>.

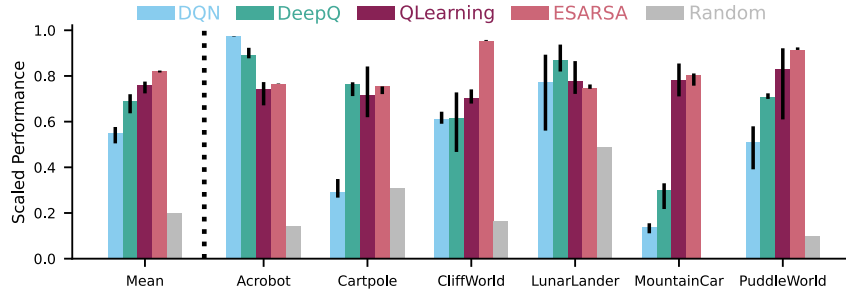


Figure 3: Applying the CHS to 10k simulated experiments. Error bars show 95% bootstrap confidence intervals. Although only three runs were used to select hyperparameters, conclusions about algorithm ranking using the CHS are perfectly consistent across all 10k experiments.

285 The SC-CHS consists of a suite of classic control environments commonly used in RL: Acrobot
 286 (Sutton, 1996), Cartpole (Barto et al., 1983; Brockman et al., 2016), Cliff World (Sutton and Barto,
 287 2018), Lunar Lander (Brockman et al., 2016), Mountain Car (Moore, 1990; Sutton, 1996), and Puddle
 288 World (Sutton, 1996). We used a discount factor of $\gamma = 0.99$ and a maximum episode length of 500
 289 steps (except in Cliff World which had a maximum length of 50 steps). We ran all algorithms for
 290 200k learning steps on each environment except Lunar Lander, where we used 250k learning steps to
 291 ensure all algorithms have reliably converged. Further details motivating this choice of environments
 292 can be found in Appendix C.1.

293 We swept over several hyperparameter settings. For all algorithms we swept eight stepsize values,
 294 $\alpha \in \{2^{-12}, 2^{-11}, \dots, 2^{-5}\}$ for the deep RL algorithms and $\alpha \in \{2^{-9}, 2^{-8}, \dots, 2^{-2}\}$ for the tile-
 295 coded algorithms. The deep RL algorithms used experience replay and target networks, so we swept
 296 over replay buffer sizes of $\{2000, 4000\}$ and target network refresh rates of $\{1, 8, 32\}$ steps where a
 297 one step refresh indicates target networks are not used. The algorithms with tile-coding learn online
 298 from the most recent sample; we select number of tiles in each tiling in $\{2, 4, 8\}$ and number of tilings
 299 in $\{8, 16, 32\}$. More details on the other hyperparameters and design decisions are in Appendix C.

300 **Variance over simulated experiments.** Here we demonstrate that the CHS provides low variance
 301 conclusions over 10k simulated experiments using the benchmark. We use bootstrap sampling
 302 to compute 10k sample means over three random seeds for every algorithm, environment, and
 303 hyperparameter to first select hyperparameters using the CHS. We then evaluate the performance
 304 of each algorithm on each environment with 250 independent runs for the selected hyperparameter
 305 settings and compare the conclusions for each of the 10k simulated experiments.

306 Figure 3 demonstrates the consistency of conclusions made using the CHS across 10k simulated
 307 experiments. Using the CHS we would rank algorithms from best to worst ESARSA, QLearning,
 308 DeepQ, and DQN on this benchmark, and this ranking was successfully detected in every experiment.
 309 Conclusions on individual environments are less consistent. This is because selecting one hyperpa-
 310 rameter across all these environments was difficult. In some runs, performance in one environment
 311 was sacrificed for the performance in the others; in another run, it was a different environment.

312 We provide more insight into the difficulty of selecting a single hyperparameter across problems, in
 313 Appendix B.1. We additionally show that the distribution of selected hyperparameters with the CHS is
 314 narrow and consistent over simulated experiments, unlike parameters chosen independently for each
 315 environment. Because conclusions are often drawn by aggregating results over environments—either
 316 formally as in the CHS or informally by counting the number of environments where an algorithm
 317 outperforms others—reporting results over a consistent and narrow distribution of hyperparameters
 318 leads towards lower variance claims and greater reproducibility. We include results selecting hyperpa-
 319 rameters according to the worst-case performance across environments in Appendix B.4; the results
 320 are highly similar, albeit slightly lower variance.

321 The cost of running a single experiment represented in Figure 3 is quite low. The deep RL algorithms
 322 test 48 hyperparameter settings at a cost of 20 minutes per run, while the tile-coded algorithms test
 323 72 settings at the cost of two minutes per run. Timings are with respect to a modern 2.1Ghz Intel
 324 Xeon processor. This comes out to a total of 1762 hours of CPU time to complete three runs for
 325 hyperparameter selection and 250 runs for evaluation, cheaper than the experiment using 10 runs and
 326 conventional per-environment tuning shown in Table 1 which cost approximately 2208 hours. The

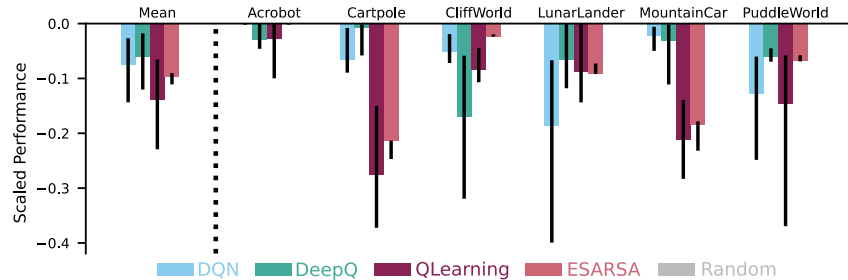


Figure 4: The change in performance for each algorithm on every environment when using the CHS versus conventional per-environment tuning. A larger drop in performance indicates a larger degree of environment overfitting when results are reported with per-environment tuning. Error bars show 95% confidence intervals over 10k bootstrap samples.

327 CHS successfully detected the correct ordering of algorithms in every trial, while the conventional
 328 per-environment tuning experiment failed to detect the correct ordering with surprising frequency.

329 **The CHS is a less optimistic measure of performance.** A motivating factor for the CHS is providing
 330 a more challenging benchmark to test across-environment insensitivity to selection of hyperparameters.
 331 Because algorithms are limited to selecting a single champion hyperparameter setting—as opposed
 332 to selecting a new hyperparameter setting for every environment—we expect a considerable drop in
 333 performance under the CHS. We evaluate the extent of this performance drop for our four algorithms
 334 by first computing near optimal parameters $\theta^* \in \Theta$ for each environment using the full 250 random
 335 seeds to obtain high confidence estimates of average performance $\mathbb{E}[N_E(G) | E, \theta^*]$. We then apply
 336 the CHS to select hyperparameters for each algorithm using three random seeds for 10k simulated
 337 experiments. We report sample estimates of $\mathbb{E}[N_E(G) | E, \theta^*] - \mathbb{E}[N_E(G) | E, \theta_{\text{CHS}}]$.

338 In Figure 4 we can see there is substantial drop in reported performance when using the CHS versus
 339 per-environment tuning. The variance is high, indicating that for some runs, the performance drop
 340 was substantial: almost 0.4 under our normalization between [0,1]. Algorithms with a large drop in
 341 performance indicate more environment-specific overfitting under per-environment tuning. Because
 342 we swept over many more hyperparameter settings for the tile-coding algorithms than for the deep
 343 RL algorithms—72 settings versus 48 settings—it is unsurprising that per-environment tuning led to
 344 far more environment overfitting in the tile-coding algorithms.

345 **Tuning on a subset of environments.** An empirical practice that is highly related to the CHS is using
 346 a subset of environments to select hyperparameters, then reporting the performance of the selected
 347 hyperparameters across an entire suite of environments. We refer to this practice as *subset-CHS*.
 348 This practice is used in the Atari suite for example, where it was suggested to use five of the 57
 349 games for hyperparameter tuning (Bellemare et al., 2013). To investigate the variance of conclusions
 350 using the subset-CHS, we run 10k simulated experiments using two of our six environments to select
 351 hyperparameters. For each of the simulated experiments, we randomly select two environments to
 352 use for hyperparameter selection. To reduce the variance, we allow each algorithm 100 runs of every
 353 hyperparameter setting on every environment to perform hyperparameter selection, then evaluate the
 354 performance on the full 250 runs for the hyperparameter selected by the subset-CHS. More results,
 355 including with varying number of runs and environments used for hyperparameter selection, can be
 356 found in Appendix B.

357 In Figure 5, we see that the ordering of algorithms is extremely high-variance—especially compared
 358 to Figure 3 which uses all six environments to select hyperparameters and only three runs. This
 359 result also illustrates large differences between individual environments, where the variance on Lunar
 360 Lander—especially for DQN—suggests that hyperparameters selected for other environments are
 361 likely to cause worse-than-random performance on Lunar Lander. At least among the four tested
 362 algorithms, it is clear that hyperparameter sensitivity is too high to use environment subselection to
 363 reduce the computational burden of hyperparameter tuning.

364 **Bias of the CHS.** Both the CHS and conventional per-environment tuning use biased sample esti-
 365 mates due to the maximization over hyperparameters. The bias due to maximization over random
 366 samples is exaggerated both as the set Θ grows and as the number of samples used to evaluate
 367 $\mathbb{E}[G | E, \theta]$ shrinks. We first estimate the true per-environment maximizing parameters θ^* and the
 368 true CHS parameter θ_{CHS}^* using 250 samples for every hyperparameter setting and environment.

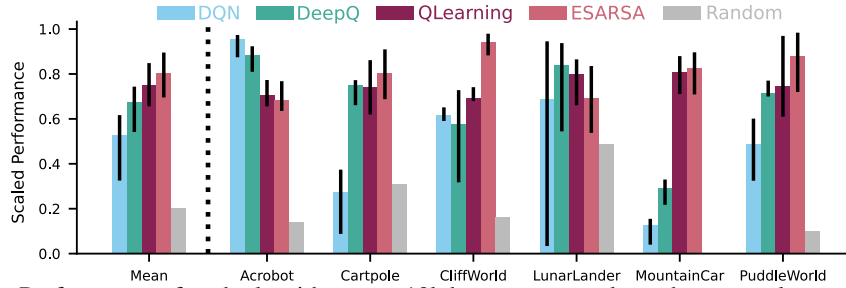


Figure 5: Performance of each algorithm over 10k bootstrap samples, where sample means are computed with 100 runs. Each bootstrap sample randomly selects two environments for hyperparameter tuning, then evaluates the chosen hyperparameter setting on all six environments with 250 runs. Error bars show 95% bootstrap confidence intervals.

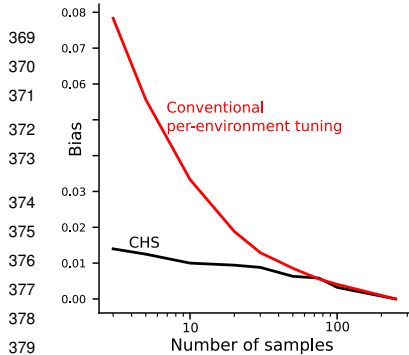


Figure 6: Bias of the CHS vs. per-environment tuning.

We then resample three samples per hyperparameter and environment to simulate an experiment using three seeds to compute sample averages, we select the maximizing parameter of these sample averages, $\hat{\theta}$, and we report $\mathbb{E}[G | E, \theta^*] - \mathbb{E}[G | E, \hat{\theta}]$. The corresponding procedure is used for the CHS.

In Figure 6, we report the bias of each procedure applied to DQN and the small control domain suite. On the vertical axis we report the bias and on the horizontal axis we show the number of random seeds used to select hyperparameters. As both procedures approach a sufficiently large number of samples to select hyperparameters, the bias of these procedures approaches zero. However when using few random seeds—for instance ten or fewer as is common in the literature—the bias of the conventional method is several times larger than that of the CHS. As a result of this overestimation bias, it is common for results in the literature to present highly optimistic results especially for algorithms with more hyperparameters.

6 A Demonstrative Example of Using the CHS

We finish with a large-scale demonstration of our benchmark across the 28 environments of the DMControl suite (Tassa et al., 2018), which we will call the DMC-CHS. For this comparison, we test an open hypothesis in the continuous control literature: does Ornstein-Uhlenbeck (OU) noise (Uhlenbeck and Ornstein, 1930) improve exploration over naive uncorrelated Gaussian noise? Autocorrelated noise for exploration was shown to be beneficial for robotics (Wawrzyński, 2015), inspiring the use of an OU noise process for DDPG (Lillicrap et al., 2016), where a single set of hyperparameters was used across 20 Mujoco environments using five seeds. Later work replaced OU noise with Gaussian noise, noting no difference in performance (Fujimoto et al., 2018; Barth-Maron et al., 2018), but without empirical support for the claim. To the best of our knowledge, no careful empirical investigation of this hypothesis has yet been published.

To apply the DMC-CHS, we first evaluate 36 hyperparameter settings with three runs per environment, for a total of 84 runs to estimate $\mathbb{E}[N_E(G) | \theta]$ for each $\theta \in \Theta$. Then we use 30 runs to evaluate the chosen θ_{CHS} for a total of 840 runs to estimate $\mathbb{E}[N_E(G) | \theta_{\text{CHS}}]$. We report the swept hyperparameters as well as the selected θ_{CHS} in Appendix B.5. We use 1k bootstrap samples to compute confidence intervals and report the overall findings in the table in Figure 7. We find that OU noise does not outperform Gaussian noise on the DMC-CHS. Considering even the extremes of the confidence intervals there is no meaningful difference in performance between these exploration methods, suggesting further runs would be unlikely to change our conclusion. We visualize the performance of OU noise on the complete suite, considering Gaussian noise experiments as a baseline in Figure 7. This visualization summarizes whether, and to what degree, OU noise improves upon Gaussian noise in each environment of the DMControl suite. In only 10 of the 28 environments, OU noise improves upon Gaussian noise, with a large improvement only in the *WalkerRun* environment. Additional results are included in Appendix B.5.

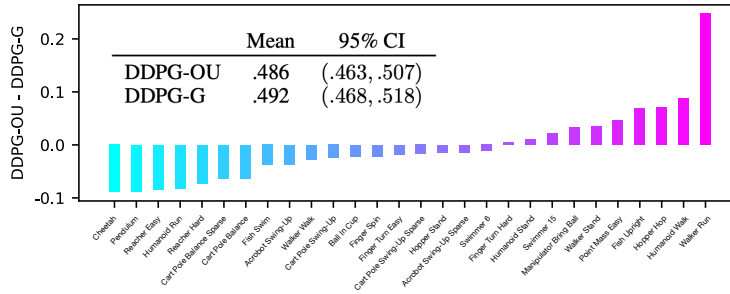


Figure 7: Comparing DDPG using OU noise vs. Gaussian noise across the DMControl suite. The inset table shows the mean performance with 95% confidence interval for the two versions of DDPG used in these experiments. Visualized in the bar plot is the performance of DDPG with OU noise, per environment in the suite, considering DDPG with Gaussian noise as a baseline.

409 **7 Conclusion**

410 In this work, we introduced a new benchmark for evaluating RL algorithms across environments,
 411 but perhaps more important are the insights we gained. Of the five algorithms we tested (including
 412 DQN and DDPG), none exhibited good performance on our CHS benchmark; aligning with the
 413 common view that we do not yet have generally applicable RL algorithms. The CHS benchmark
 414 produces reliable conclusions with only three runs in the preliminary sweep while providing a new
 415 challenging aspect to small computationally-cheap environments, allowing small university labs and
 416 tech giants alike to conduct rigorous and meaningful comparisons. Finally, prior work has disagreed
 417 on the benefit of using OU or Gaussian noise in DDPG on Mujoco-based environments. Perhaps
 418 some combination of too few runs, using default hyperparameters, or problematic environment sub-
 419 selection yielded conflicting results. Our results with CHS suggest there is no significant performance
 420 difference across a suite of 28 Mujoco environments, putting this debate to bed. The CHS benchmark
 421 can play a role uncovering falsehoods and resolving disputes.

422 The CHS is a general procedure for evaluating performance across environments. We provide two
 423 example instantiations of the CHS, the SC-CHS for discrete action control on small domains and
 424 the DMC-CHS for continuous control on large simulated environments, however the CHS can also
 425 be extended to use arbitrary environment sets to allow targeted evaluation across environments with
 426 certain desirable properties. For example, the taxonomies of Atari games identified in Bellemare
 427 et al. (2016), the off-policy evaluation environments used in Sutton et al. (2009), or the taxonomy
 428 of exploration environments from Yasui et al. (2019) are each sets of environments that have been
 429 previously identified and used across the literature. Applying the CHS to any one of the environment
 430 sets provides a new challenge, and in some small way can push us towards generally applicable RL
 431 agents.

432 References

- 433 T. W. Archibald, K. I. M. McKinnon, and L. C. Thomas. On the generation of markov decision
434 processes. *Journal of the Operational Research Society*, 1995.
- 435 André M.S. Barreto, Heder S. Bernardino, and Helio J.C. Barbosa. Probabilistic performance profiles
436 for the experimental evaluation of stochastic algorithms. *Conference on Genetic and Evolutionary*
437 *Computation*, 2010.
- 438 Gabriel Barth-Marón, Matthew W. Hoffman, David Budden, Will Dabney, Dan Horgan, Dhruva TB,
439 Alistair Muldal, Nicolas Heess, and Timothy Lillicrap. Distributed Distributional Deterministic
440 Policy Gradients. *International Conference on Learning Representations*, 2018.
- 441 Andrew G. Barto, Richard S. Sutton, and Charles W. Anderson. Neuronlike adaptive elements that can
442 solve difficult learning control problems. *IEEE Transactions on Systems, Man, and Cybernetics*,
443 1983.
- 444 Charles Beattie, Joel Z. Leibo, Denis Teplyashin, Tom Ward, Marcus Wainwright, Heinrich Küttler,
445 Andrew Lefrancq, Simon Green, Víctor Valdés, and Amir Sadik. Deepmind lab. *arXiv preprint*
446 *arXiv:1612.03801*, 2016.
- 447 M. G. Bellemare, Y. Naddaf, J. Veness, and M. Bowling. The Arcade Learning Environment: An
448 Evaluation Platform for General Agents. *Journal of Artificial Intelligence Research*, 2013.
- 449 Marc Bellemare, Sriram Srinivasan, Georg Ostrovski, Tom Schaul, David Saxton, and Remi Munos.
450 Unifying count-based exploration and intrinsic motivation. *Advances in neural information*
451 *processing systems*, 2016.
- 452 Greg Brockman, Vicki Cheung, Ludwig Pettersson, Jonas Schneider, John Schulman, Jie Tang, and
453 Wojciech Zaremba. Openai gym. *arXiv preprint arXiv:1606.01540*, 2016.
- 454 Cédric Colas, Olivier Sigaud, and Pierre-Yves Oudeyer. How Many Random Seeds? Statistical
455 Power Analysis in Deep Reinforcement Learning Experiments. *arXiv:1806.08295*, 2018.
- 456 Logan Engstrom, Andrew Ilyas, Shibani Santurkar, Dimitris Tsipras, Firdaus Janoos, Larry Rudolph,
457 and Aleksander Ma. Implementation Matters In Deep Policy Gradients: A Case Study On PPO
458 and TRPO. *International Conference on Learning Representations*, 2019.
- 459 Lasse Espeholt, Hubert Soyer, Remi Munos, Karen Simonyan, Volodymyr Mnih, Tom Ward, Yotam
460 Doron, Vlad Firoiu, Tim Harley, Iain Dunning, Shane Legg, and Koray Kavukcuoglu. IMPALA:
461 Scalable Distributed Deep-RL with Importance Weighted Actor-Learner Architectures. *Interna-*
462 *tional Conference on Machine Learning*, 2018.
- 463 Scott Fujimoto, Herke Van Hoof, and David Meger. Addressing function approximation error in
464 actor-critic methods. *International Conference on Machine Learning*, 2018.
- 465 Peter Henderson, Riashat Islam, Philip Bachman, Joelle Pineau, Doina Precup, and David Meger.
466 Deep Reinforcement Learning that Matters. *AAAI*, 2018.
- 467 Matt Hoffman, Bobak Shahriari, John Aslanides, Gabriel Barth-Marón, Feryal Behbahani, Tamara
468 Norman, Abbas Abdolmaleki, Albin Cassirer, Fan Yang, Kate Baumli, Sarah Henderson, Alex
469 Novikov, Sergio Gómez Colmenarejo, Serkan Cabi, Caglar Gulcehre, Tom Le Paine, Andrew
470 Cowie, Ziyu Wang, Bilal Piot, and Nando de Freitas. Acme: A Research Framework for Distributed
471 Reinforcement Learning. *arXiv:2006.00979*, 2020.
- 472 Max Jaderberg, Volodymyr Mnih, Wojciech Marian Czarnecki, Tom Schaul, Joel Z. Leibo, David
473 Silver, and Koray Kavukcuoglu. Reinforcement Learning with Unsupervised Auxiliary Tasks.
474 *International Conference on Learning Representations*, 2016.
- 475 Scott M. Jordan, Yash Chandak, Daniel Cohen, Mengxue Zhang, and Philip S. Thomas. Evaluating
476 the Performance of Reinforcement Learning Algorithms. *International Conference on Machine*
477 *Learning*, 2020.
- 478 Diederik P Kingma and Jimmy Ba. Adam: A Method for Stochastic Optimization. *International*
479 *Conference on Learning Representations*, 2015.

480 Timothy P. Lillicrap, Jonathan J. Hunt, Alexander Pritzel, Nicolas Heess, Tom Erez, Yuval Tassa,
481 David Silver, and Daan Wierstra. Continuous control with deep reinforcement learning. *International Conference on Learning Representations*, 2016.
482

483 Ashique Rupam Mahmood, Hado Van Hasselt, and Richard S. Sutton. Weighted importance sampling
484 for off-policy learning with linear function approximation. *Advances in Neural Information*
485 *Processing Systems*, 2014.

486 Volodymyr Mnih, Koray Kavukcuoglu, David Silver, Alex Graves, Ioannis Antonoglou, Daan
487 Wierstra, and Martin Riedmiller. Playing Atari with Deep Reinforcement Learning. 2013.

488 Andrew William Moore. *Efficient Memory-Based Learning for Robot Control*. PhD thesis, University
489 of Cambridge, 1990.

490 Johan S. Obando-Ceron and Pablo Samuel Castro. Revisiting Rainbow: Promoting more insightful
491 and inclusive deep reinforcement learning research. *International Conference on Machine Learning*,
492 2021.

493 Andrew Patterson, Adam White, Sina Ghiassian, and Martha White. A Generalized Projected
494 Bellman Error for Off-policy Value Estimation in Reinforcement Learning. *In submission*, 2021.

495 Joelle Pineau, Philippe Vincent-Lamarre, Koustuv Sinha, Vincent Larivière, Alina Beygelzimer,
496 Florence d’Alché-Buc, Emily Fox, and Hugo Larochelle. Improving Reproducibility in Machine
497 Learning Research (A Report from the NeurIPS 2019 Reproducibility Program). *arXiv:2003.12206*,
498 2020.

499 Antonin Raffin, Ashley Hill, Maximilian Ernestus, Adam Gleave, Anssi Kanervisto, and Noah
500 Dormann. Stable Baselines3. DLR-RM, 2019.

501 Tom Schaul, John Quan, Ioannis Antonoglou, and David Silver. Prioritized Experience Replay.
502 *International Conference on Learning Representations*, 2016.

503 Harm Seijen and Rich Sutton. True online TD (λ). In *International Conference on Machine*
504 *Learning*, 2014.

505 Richard S. Sutton. Generalization in reinforcement learning: Successful examples using sparse coarse
506 coding. *Advances in Neural Information Processing Systems*, 1996.

507 Richard S. Sutton and Andrew G. Barto. *Reinforcement Learning: An Introduction*. MIT Press, 2018.

508 Richard S. Sutton, Hamid Reza Maei, Doina Precup, Shalabh Bhatnagar, David Silver, Csaba
509 Szepesvári, and Eric Wiewiora. Fast gradient-descent methods for temporal-difference learning
510 with linear function approximation. *International Conference on Machine Learning*, 2009.

511 Adrien Ali Taïga, William Fedus, Marlos C. Machado, Aaron Courville, and Marc G. Bellemare.
512 Benchmarking Bonus-Based Exploration Methods on the Arcade Learning Environment. *Exploration in Reinforcement Learning Workshop, ICML*, 2019.
513

514 Yuval Tassa, Yotam Doron, Alistair Muldal, Tom Erez, Yazhe Li, Diego de Las Casas, David Budden,
515 Abbas Abdolmaleki, Josh Merel, Andrew Lefrancq, Timothy Lillicrap, and Martin Riedmiller.
516 DeepMind Control Suite. *arXiv:1801.00690*, 2018.

517 George E. Uhlenbeck and Leonard S. Ornstein. On the theory of the Brownian motion. *Physical*
518 *review*, 1930.

519 Hado Van Hasselt, Arthur Guez, and David Silver. Deep reinforcement learning with double q-
520 learning. In *Proceedings of the AAAI Conference on Artificial Intelligence*, volume 30, 2016.

521 Hado van Hasselt, Matteo Hessel, and John Aslanides. When to use parametric models in reinforce-
522 ment learning? *arXiv:1906.05243*, 2019.

523 Ziyu Wang, Tom Schaul, Matteo Hessel, Hado van Hasselt, Marc Lanctot, and Nando de Freitas.
524 Dueling Network Architectures for Deep Reinforcement Learning. *International Conference on*
525 *Machine Learning*, 2016.

- 526 Paweł Wawrzyński. Control Policy with Autocorrelated Noise in Reinforcement Learning for
527 Robotics. *International Journal of Machine Learning and Computing*, 2015.
- 528 Adam White and Martha White. Investigating practical linear temporal difference learning. *International Conference on Autonomous Agents and Multi-Agent Systems*, 2016.
- 530 Shimon Whiteson, Brian Tanner, Matthew E. Taylor, and Peter Stone. Generalized domains for
531 empirical evaluations in reinforcement learning. *Workshop on Evaluation Methods for Machine
532 Learning at ICML*, 2009.
- 533 Niko Yasui, Sungsu Lim, Cam Linke, Adam White, and Martha White. An Empirical and Conceptual
534 Categorization of Value-based Exploration Methods. *Exploration in Reinforcement Learning
535 Workshop, ICML*, 2019.

536 **Checklist**

- 537 1. For all authors...
- 538 (a) Do the main claims made in the abstract and introduction accurately reflect the paper's
539 contributions and scope? [Yes]
- 540 (b) Did you describe the limitations of your work? [Yes] Section 4 discusses our relation-
541 ship to Jordan et al. (2020) and that their work allows further quantitative evaluation of
542 the difficulty in choosing hyperparameters.
- 543 (c) Did you discuss any potential negative societal impacts of your work? [N/A]
- 544 (d) Have you read the ethics review guidelines and ensured that your paper conforms to
545 them? [Yes]
- 546 2. If you are including theoretical results...
- 547 (a) Did you state the full set of assumptions of all theoretical results? [N/A]
- 548 (b) Did you include complete proofs of all theoretical results? [N/A]
- 549 3. If you ran experiments (e.g. for benchmarks)...
- 550 (a) Did you include the code, data, and instructions needed to reproduce the main experi-
551 mental results (either in the supplemental material or as a URL)? [Yes]
- 552 (b) Did you specify all the training details (e.g., data splits, hyperparameters, how they
553 were chosen)? [Yes]
- 554 (c) Did you report error bars (e.g., with respect to the random seed after running experi-
555 ments multiple times)? [Yes]
- 556 (d) Did you include the total amount of compute and the type of resources used (e.g.,
557 type of GPUs, internal cluster, or cloud provider)? [Yes] Appendix A details the
558 computational resources required for this paper.
- 559 4. If you are using existing assets (e.g., code, data, models) or curating/releasing new assets...
- 560 (a) If your work uses existing assets, did you cite the creators? [Yes]
- 561 (b) Did you mention the license of the assets? [N/A]
- 562 (c) Did you include any new assets either in the supplemental material or as a URL? [N/A]
- 563
- 564 (d) Did you discuss whether and how consent was obtained from people whose data you're
565 using/curating? [N/A]
- 566 (e) Did you discuss whether the data you are using/curating contains personally identifiable
567 information or offensive content? [N/A]
- 568 5. If you used crowdsourcing or conducted research with human subjects...
- 569 (a) Did you include the full text of instructions given to participants and screenshots, if
570 applicable? [N/A]
- 571 (b) Did you describe any potential participant risks, with links to Institutional Review
572 Board (IRB) approvals, if applicable? [N/A]
- 573 (c) Did you include the estimated hourly wage paid to participants and the total amount
574 spent on participant compensation? [N/A]

575 A Ethical considerations

576 Because the Cross-environment Hyperparameter Setting Benchmark is applied to experimenter-
577 picked domains, it inherits the biases and ethical considerations of the studied domains. However,
578 the primary goal of the CHS is to reduce algorithm design decisions which lead to overfitting to
579 specific attributes of studied domains. An example could be the use of layer-normalization within
580 neural networks, which highly disproportionately favor pixel-based domains. If the CHS utilized
581 only pixel-based domains, the results would still follow the bias of the experiment designer; however
582 if even a single non-pixel domain was included in the benchmark, the biased design decision to
583 use layer-normalization would negatively impact the outcome of this particular algorithm on this
584 benchmark. Previous empirical practices are more likely to permit this form of biased design due to
585 statistical noise or domain subselection.

586 A major motivation for this paper is to advocate that meaningful and sound experiments in RL are
587 achievable at an inclusive and low cost. Running a complete experiment with four algorithms on the
588 six small control environments used in Section 5 would cost approximately \$40 USD at current AWS
589 EC2 prices and would complete in approximate two days. This experiment is complete, sound, and
590 provides a meaningful ranking of four comparison algorithms; even detecting performance differences
591 across minute algorithmic differences. However, the CHS is not perfectly resilient to gaming with
592 extensive hyperparameter tuning. Consider the highly common scenario where we wish to advocate
593 for one algorithm over competitive baselines, then performing extensive tuning or multiple iterations
594 of tuning with the CHS still gives advantage to labs with greater access to resources.

595 For the studies performed in Section 5, we required far more compute than would be typical of
596 a study utilizing the CHS. To evaluate the effectiveness of the CHS required sufficient data to
597 simulate repeated applications of CHS on new data. Our results were obtained using a cloud CPU
598 cluster using approximately 2000 Intel Xeon cores running at 2.1Ghz simultaneously. We utilized
599 approximately 2.4 CPU years to collect the small control experiments data used for this study, with
600 all post-processing, analysis, and plotting done locally on a laptop. The large demonstration on the
601 DMC-CHS required approximately 1.3 GPU years of compute.

602 B Additional Results

603 In this section, we provide additional results of experiments run in Section 5. For these results, we
604 use the same experimental setup as in Section 5, namely we form a dataset of 250 runs of every
605 hyperparameter setting, environment, and algorithm tuple. From this extensive dataset, we use
606 bootstrap resampling to simulate experimental trials using the CHS. We start by investigating a slice
607 of the sample distributions from which we perform resampling, then we provide additional results
608 demonstrating the high variance of conclusions drawn from tuning on a subset of environments.

609 B.1 Distribution of selected hyperparameters.

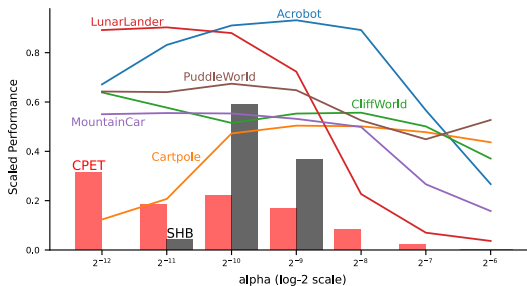


Figure 8: Bars represent the distribution of selected stepsizes using conventional per-environment tuning (**red**) or when using the CHS (**black**). Lines show the sensitivity curves for each environment. Confidence regions around the sensitivity curves are negligibly small and are not visible when plotted.

610 We show that the distribution of selected hyperparameters with the CHS is narrow and consistent
611 over simulated experiments, unlike parameters chosen independently for each environment. Because
612 conclusions are often drawn by aggregating results over environments—either formally as in the
613 CHS or informally by counting wins—reporting results over a consistent and narrow distribution of
614 hyperparameters leads towards lower variance claims and greater reproducibility.

615 Figure 8 demonstrates the wide range of stepsizes used to draw conclusions using repeated appli-
616 cations of the conventional per-environment tuning approach and the relatively narrow range used

617 by repeated applications of the CHS. DQN does not have a consistently good stepsize setting that
 618 solves every environment, or even a majority of environments. Several sensitivity curves have fairly
 619 opposite performance for a given stepsize, demonstrating the difficulty in picking a single stepsize
 620 with which to evaluate DQN.

621 Previous works generally investigate sensitivity over hyperparameters on each environment individu-
 622 ally. This within-environment investigation empirically shows the deviation in performance of an
 623 algorithm if different settings of a hyperparameter were used, indicating the difficulty of selecting
 624 hyperparameters for just that environment. Our goal is slightly different. We seek to measure the
 625 difficulty of selecting hyperparameters across multiple environments. Consider DQN’s sensitivities
 626 in Figure 8. By looking at Acrobot, Cartpole, and Mountain Car—a commonly used suite of classic
 627 control environments—we might conclude that DQN is across-environment insensitive because it
 628 is simultaneously within-environment insensitive for these environment. However, expanding our
 629 investigation by including Puddle World we see again that DQN is within-environment insensitive,
 630 but across-environment highly sensitive; Cartpole and Puddle World have very few overlapping good
 631 stepsizes. Adding the Lunar Lander environment and it is clear that DQN is not within-environment
 632 insensitive, and as such is highly unlikely to be across-environment insensitive as well.

633 B.2 Tuning on a subset

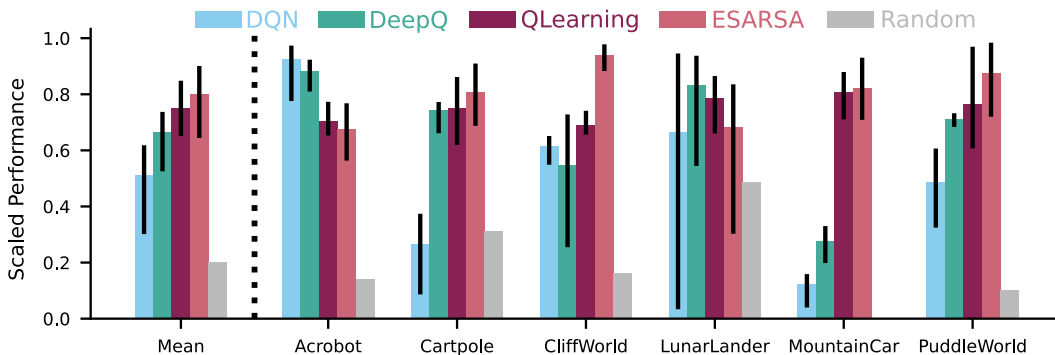


Figure 9: Outcome of the CHS when using **two** randomly selected domains to tune hyperparameters, then evaluating hyperparameters on all six domains. Each of the 10k simulated experiments use three seeds to select hyperparameters, then 250 seeds to evaluate performance.

634 In Section 5, we investigate the impact of using a subset of environments to tune hyperparameters
 635 while reporting results on the full set of environments. We demonstrated the high variance of
 636 conclusions using two randomly selected domains for each simulated experiment and using 100
 637 random seeds to pick hyperparameters. In Figure 9, we demonstrate even greater variance in
 638 conclusions when using only three seeds to pick hyperparameters; using a consistent number of seeds
 639 as the rest of our prior evaluation. In this setting, the correct ordering of algorithms is detected in only
 640 approximately 40% of experiments, with distinguishing between QLearning and ESARSA providing
 641 the largest source of error. Notice also that the variance in Lunar Lander for DQN is such that the
 642 95% confidence interval about the mean states that the true mean is 95% likely to lie in the interval
 643 [0.05, 0.98] where the performance metric is bounded between 0 and 1. In other words, evaluating
 644 the performance of DQN on Lunar Lander using this experimental design is effectively useless.

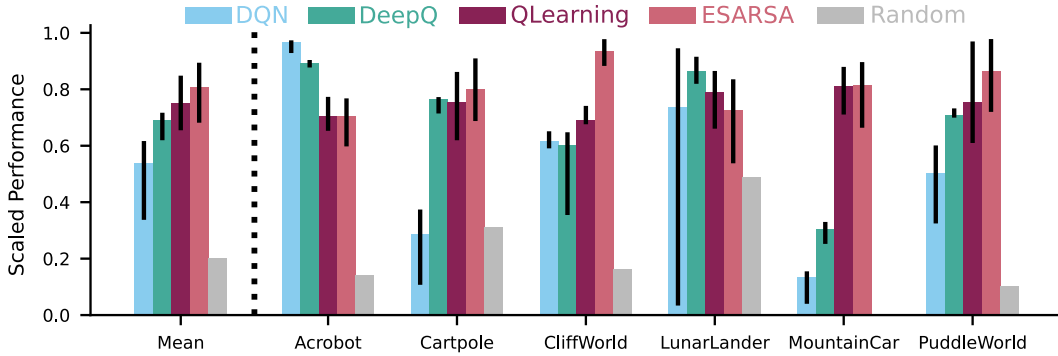


Figure 10: Outcome of the CHS when using **three** randomly selected domains to tune hyperparameters. Each of the 10k simulated experiments use 100 seeds to select hyperparameters, then 250 seeds to evaluate performance.

645 We continue our investigation of using a subset of environments to select hyperparameters in Fig-
 646 ures 10 and 11 where we use three of six environments and four of six environments respectively.
 647 In both figures we use 100 random seeds to select hyperparameters, consistent with Figure 5 in
 648 Section 5. In Figure 10, the variance in overall conclusions is notably smaller than when using two of
 649 six environments to select hyperparameters. This experimental design allows distinguishing between
 650 DQN and DeepQ reliably, but still fails to distinguishing the performance of QLearning and ESARSA.
 651 The variance of DQN on Lunar Lander still provides a comically large confidence region.

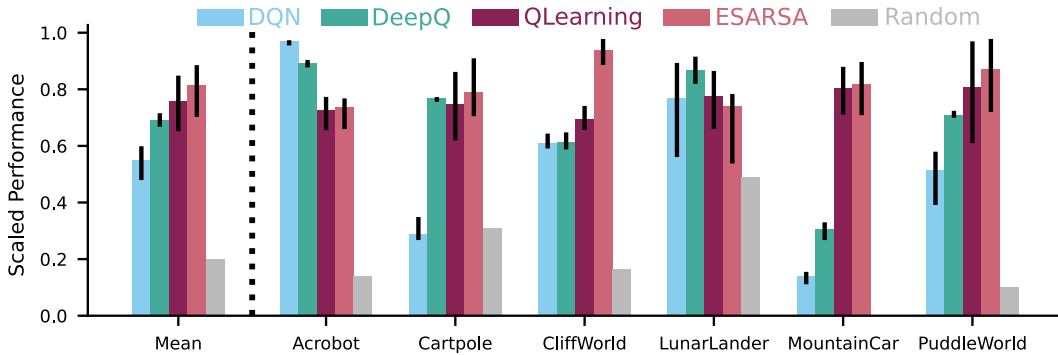


Figure 11: Outcome of the CHS when using **four** randomly selected domains to tune hyperparameters. Each of the 10k simulated experiments use 100 seeds to select hyperparameters, then 250 seeds to evaluate performance.

652 Figure 11 uses four of six environments with 100 random seeds for each hyperparameter setting
 653 to select hyperparameters. The confidence region around DQN and DeepQ indicates a clear and
 654 meaningful ordering in the performance of the deep RL algorithms across these environments. Still
 655 QLearning and ESARSA remain indistinguishable. The variance on individual environments is
 656 sensible, allowing some conclusions to be drawn with confidence especially when comparing DeepQ
 657 and DQN. We point out that the computational savings of using four of six environments is entirely
 658 negated by the number of random seeds required to select hyperparameters in this experimental design,
 659 calling to question the utility of subselecting environments. This suggests that this experimental
 660 design is likely not yet appropriate for use in RL due to high variance in conclusions—at least until
 661 future algorithm development yields algorithms with significantly less across-environment sensitivity.

662 B.3 Performance distributions

663 Figure 12 demonstrates that the shapes of the performance distributions are highly inconsistent across
 664 environment and choice of stepsize parameter. It is clear that assuming normality of the data is in
 665 general impossible, even for these simple algorithms and small domains. Experiments that use only a
 666 small number of random seeds—especially when maximizing over repeated trials, or cherry-picking
 667 over completed results—are highly unlikely to capture the bimodality and skew present in many

668 of these distributions. Consider, for instance, the Lunar Lander environment with DQN. Using a
 669 small number of random seeds—for instance three—it is highly unlikely that the long-tail of the
 670 distribution for stepsize $\alpha = 2^{-9}$ is accurately captured. Instead, the most likely outcome is that the
 671 mean of the high-performing mode is reported, ignoring the instability of the DQN algorithm.

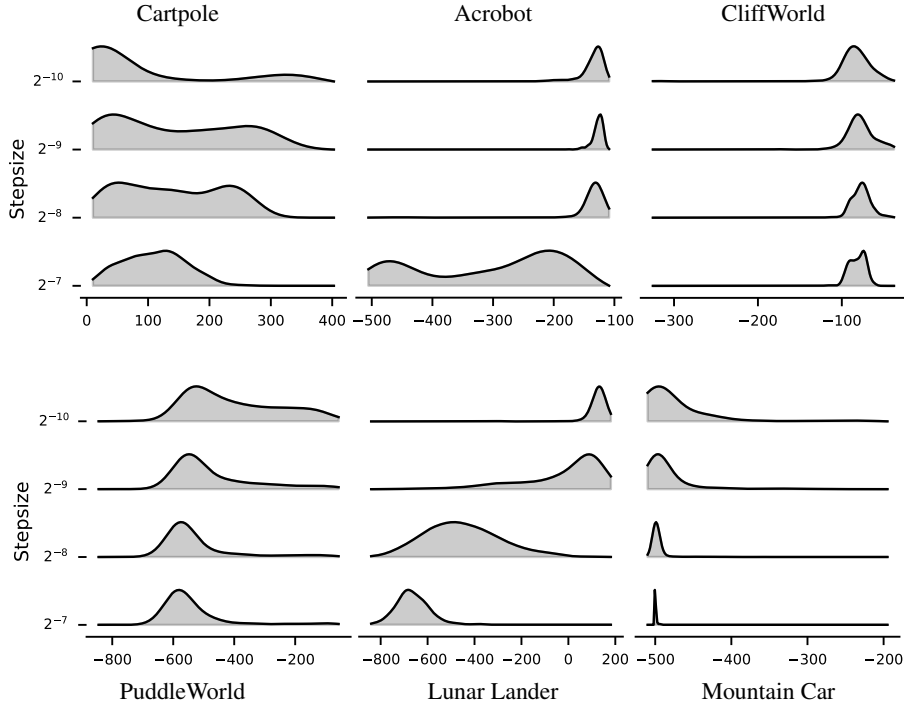


Figure 12: Various slices of $\mathbb{P}(G | E, \theta)$ for all $E \in \mathcal{E}$ and a subset of Θ for the DQN algorithm. Every distribution is estimated with a Gaussian kernel density estimator and 250 samples. The supports for the distributions are computed by finding the absolute min and max run for the visualized hyperparameter settings. This means, for instance, that at least one run shown on Mountain Car achieved a performance of approximately -200 return, but was such a low probability event it is not visible in these plots.

672 B.4 Results when using worst-case performance across environments

673 The prior evaluations of the CHS all estimated $\mathbb{E}[N_E(G) | \theta_{\text{CHS}}]$ with hyperparameters selected to maximize this expectation. However, we could instead select hyperparameters according to other statistics, for instance those with best performance on the worst-case environment, $\max_{\theta} \min_E \mathbb{E}[N_E(G) | E, \theta]$. We demonstrate in Figure 13 the outcome of the CHS when θ_{CHS} is selected according to maximizing performance on the worst-case environment. Note the nested optimization means the environment chosen may be different per algorithm and even per hyperparameter setting.
 674
 675
 676
 677
 678
 679

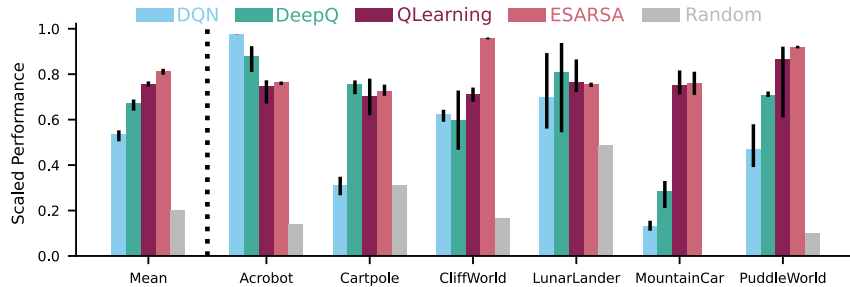


Figure 13: Performance of each algorithm over 10k bootstrap samples, where sample means are computed with 3 runs. Hyperparameters are selected for maximizing performance of the worst-case environment. Error bars show 95% bootstrap confidence intervals.

680 In general, the variability of conclusions made over 10k simulated applications of the CHS is much
681 smaller than when estimating the mean over environments, as shown in Figure 13. We still see high
682 variance in the Lunar Lander environment for the two DRL algorithms, suggesting still high sensitivity
683 to the chosen hyperparameters. Because the worst-case environment for DQN is Cartpole for many
684 choices of hyperparameter, likewise Mountain Car for DeepQ, it is likely that these environments
685 largely dictate the choice of hyperparameter without regard for performance on Lunar Lander. Under
686 this worst-case benchmark, algorithm development improving the performance of DQN on Cartpole
687 would be highly rewarded while development slightly improving its performance on Acrobot would
688 have no effect. This is unlike conventional benchmarks where minute improvements on already
689 well-solved problems are rewarded similarly to large improvements on challenging problems.

690 B.5 DMControl demonstration

691 Figure 14 shows the per-environment performance for DDPG using both OU noise and Gaussian
692 noise evaluated using 30 runs of the θ_{CHS} setting. In most cases, the performance of each exploration
693 method was not statistically significantly different. Although there is a large difference in the
694 WalkerRun environment, we point out this may be due to the CHS trading-off performance on other
695 environments in order to pick a single hyperparameter setting; without explicit per-environment
696 experimentation this remains unclear.

697 C Further Experimental Details

698 In this section we include all experimental details used in Section 5, descriptions of the environments
699 used are included in Appendix C.1, and details about the DMControl demonstration from Section 6
700 are included in Appendix C.2.

701 The tile-coded agents both learn directly from the most recent observations without the use of a replay
702 buffer. We use stochastic gradient descent to optimize the agents, with stepsizes scaled by the number
703 of active tiles in the representation—equal to the number of tilings used by the tile-coder except in
704 the special case of Lunar Lander. Like their deep RL counterparts, we use ϵ -greedy policies to train
705 the tile-coding agents with $\epsilon = 0.1$ for all experiments.

706 C.1 Small control environments

707 In this section, we describe the environments used to evaluate the CHS in Section 5. Our goal in
708 environment selection was to highlight differences between the demonstrative algorithms, while
709 simultaneously using small enough environments to feasibly collect an extensive dataset to justify
710 our experiment design. Because all of our demonstrative algorithms use ϵ -greedy action selection as
711 their sole form of exploration, we avoid environments where exploration is a particular challenge as
712 this would not help in distinguishing between algorithms.

713 For the Acrobot environment (Sutton, 1996), we use the implementation from Brockman et al.
714 (2016). Acrobot has a medium-sized observation dimension with six observable values, making
715 feature representation challenging for tile-coding agents. Similarly, we include the Lunar Lander
716 environment (Brockman et al., 2016) as its observation dimension is too large for tile-coding to
717 successfully generate a useful representation. Lunar Lander additionally has a highly shaped reward
718 function, making the learning dynamics very different from all other included environments.

719 For the Cartpole (Barto et al., 1983) and Mountain Car (Moore, 1990) environments, we likewise
720 use the implementation from Brockman et al. (2016). Both environments have a small observation
721 dimension, making the feature representation amenable to tile-coding. Prior results have suggested a
722 stark difference in performance between DQN and DeepQ on these environments, suggesting their
723 utility in distinguishing between algorithms.

724 Lastly, CliffWorld (Sutton and Barto, 2018) and PuddleWorld (Sutton, 1996) are both two dimensional
725 gridworlds. The small observation dimension is easier for tile-coding agents to represent and presents
726 a challenge for neural network based agents. CliffWorld is commonly used to showcase large
727 differences between on-policy and off-policy algorithms (Sutton and Barto, 2018), making it a good
728 choice for differentiating between the three Q-learning based agents and ESARSA. Additionally, the
729 sudden large negative reward obtained from falling off the cliff could cause high variance updates for

730 mean squared based algorithms, suggesting a slight advantage for DQN. PuddleWorld uses a dense
731 reward function with shaping, making it similar to Lunar Lander.

732 C.2 Details about DM Control demonstration

733 The demonstration in Section 6 was generated using the Acme codebase of RL algorithms (Hoffman
734 et al., 2020). We reuse as much code from Acme as possible to maintain similarity in empirical setup
735 and computational cost with prior works coming from this lab, e.g Tassa et al. (2018); Lillicrap et al.
736 (2016); Barth-Maron et al. (2018). We use the default hyperparameters and network architectures for
737 all experiments and environments as in Acme, except for those which we swept. We used 3 random
738 seeds for each environment and hyperparameter setting to select hyperparameters according to the
739 CHS, then we perform an additional 30 runs to evaluate θ_{CHS} .

740 For the hyperparameter sweep, we evaluated stepsize $\alpha \in \{10^{-4}, 10^{-3}, 10^{-2}\}$ for the critic and
741 $\eta \in \{10^0, 10^{-1}, 10^{-2}\}$ where $\beta = \eta\alpha$ and β is the stepsize for the actor network. We use the
742 ADAM optimizer with default parameters. We additionally swept over target network types, using
743 either Polyak averaging with moving average parameter $\beta_{tn} = 0.001$ or a hard refresh every 100
744 steps. Finally, we swept the standard deviation of the exploration noise $\sigma \in \{0.05, 0.1\}$ —a slight
745 deviation in ranges tested by previous works as we noticed $\sigma > 0.1$ was rarely a good choice on most
746 environments, but $\sigma < 0.1$ was often required to obtain better than random performance on several
747 environments (e.g. Acrobot).

748 All experiments run for a maximum of 300k learning steps and use an infinite replay buffer. On every
749 environment interaction after the first 1000 steps, the DDPG agent made a mini-batch update using a
750 mini-batch size of 64. To maintain consistency with prior works, a soft-termination occurs after 1000
751 steps in an episode.

752 Finally, we include the hyperparameters selected by the DMC-CHS. Both DDPG and DDPG-OU
753 selected the same hyperparameters when using the DMC-CHS. Defaults taken from the Acme
754 codebase (Hoffman et al., 2020), as was the code implementation.

```
{  
  "max_steps": 300000,  
  "metaParameters": {  
    "actor_stepsize_scale": 1.0,  
    "critic_stepsize": 1e-4,  
    "discount": 0.99,  
    "target_update": 0.001,  
  
    "buffer_size": "infinite",  
    "min_replay_size": 1000,  
    "steps_per_update": 1,  
755    "batch": 64,  
  
    "n_step": 1,  
    "sigma": 0.1,  
    "theta": 0.15,  
    "mu": 0.0,  
    "clipping": false,  
  
    "obs_weights": [[400, 400]],  
    "policy_weights": [[300, 200]],  
    "critic_weights": [[400, 300]],  
  }  
}
```

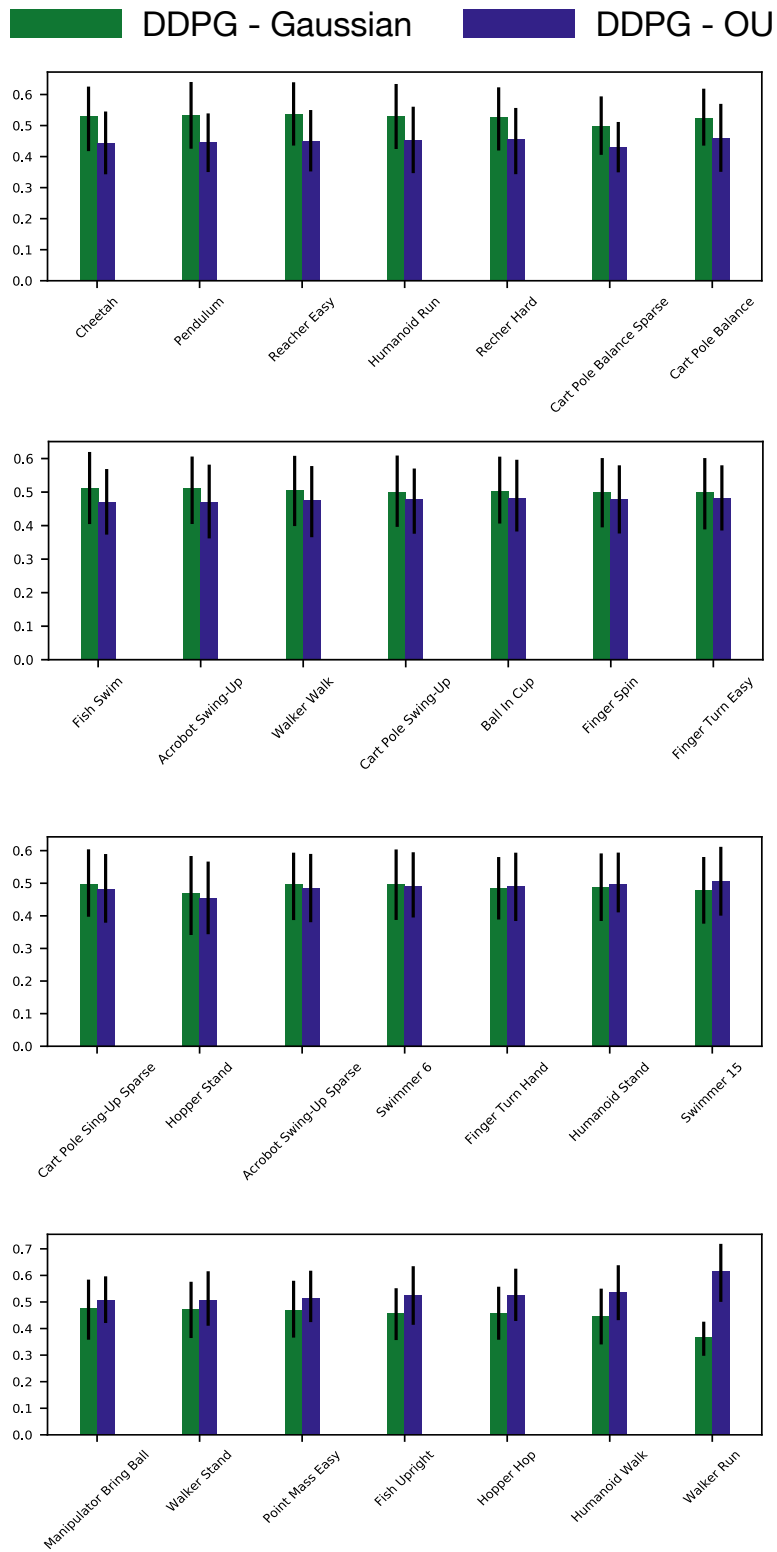


Figure 14: Per-environment performance differences for every environment in the DMControl suite. Error bars show 95% confidence intervals using 1k bootstrap samples. Performance is averaged over 30 independent runs.